ELSEVIER

Journal of Magnetism and Magnetic Materials 223 (2001) 253–260

Journal of magnetism and magnetic materials

www.elsevier.com/locate/jmmm

Spiral spin structures of RMn_6Ge_6 (R = Gd, Tb, Dy)

M.T. Kelemen[a], P. Rösch[a], E. Dormann[a,*], K.H.J. Buschow[b]

[a] *Physikalisches Institut, Universität Karlsruhe (TH), D-76128 Karlsruhe, Germany*

[b] *Van der Waals-Zeeman Laboratorium, Universiteit van Amsterdam, Postbus 20215, NL-1000 HE, Amsterdam, Netherlands*

Received 18 July 2000; received in revised form 25 October 2000

Abstract

The field dependences of the magnetic moment of several $Gd_XY_{1-X}Mn_6Ge_6$ compounds have been analysed by a mean-field theory of several spin structures. The assumption of spiral spin structures at low temperatures in these compounds has been confirmed. In addition to this, the magnetic phase diagrams of $TbMn_6Ge_6$ and $DyMn_6Ge_6$ have been deduced from magnetisation measurements of powder samples. In contrast to $GdMn_6Ge_6$, the crystal fields of these compounds produce a variety of additional spin phases.

PACS: 75.10.Hk; 75.25. + z

Keywords: Magnetic phase diagram; Intermetallic compound; Rare earths; Manganese; Mean-field model

1. Introduction

In recent years, intermetallic layer-like compounds containing localised rare-earth (R) moments and the 3d-transition element manganese have been investigated by magnetisation measurements and neutron diffraction [1,2]. The phase diagrams of $Gd_XY_{1-X}Mn_6Ge_6$ consists of a paramagnetic, a ferrimagnetic, a canted ferrimagnetic and a phase characterised by a very small macroscopic magnetisation [3,7]. With a combination of macroscopic magnetisation data and the local information obtained from NMR, this phase has been analysed to be a flat spiral spin structure. This indirect analysis method could be confirmed by a detailed analytical simulation of the field dependent magnetisation curves in Ref. [7]. So based on a theory of Refs. [4,5], this work will present a method to explain the field dependence of the magnetisation of $Gd_XY_{1-X}Mn_6Ge_6$. In addition to this, the phase diagrams of $TbMn_6Ge_6$ and $DyMn_6Ge_6$ have been established by magnetisation measurements to compare with the data of neutron scattering.

The RMn_6Ge_6 crystallises in the $HfFe_6Ge_6$-type structure (space group P6/mmm) that can be described as being built of alternate (0 0 1) layers containing Gd and Mn, respectively. Whereas the Gd atoms build hexagonal planes (H), Mn atoms build Kagome nets (K) stacked along the *c*-axis with the sequence … KHKKHK … [2]. Two Mn planes and one Gd plane build a three-layer stack called trilayer in this report.

* Corresponding author. Tel.: + 49-721-608-3455; fax + 49-721-608-6103.

E-mail address: edo@piobelix.physik.uni-karlsruhe.de (E. Dormann).

0304-8853/01/$ - see front matter
PII: S0304-8853(00)01269-5

All magnetic measurements in the temperature range 2–750 K were performed on powder samples using a commercial SQUID magnetometer with magnetic fields up to 55 kOe.

2. Field dependence of $Gd_XY_{1-X}Mn_6Ge_6$

Rare-earth compounds are distinguished by a large number of different magnetic spiral structures. The RKKY-interaction between localised 4f-moments and polarised conduction electrons characterised through long-range and oscillatory behaviour is a necessary condition for the existence of spiral spin structures. Other metals rarely show such complicated magnetic behaviour. Starting with a relatively simple approach in the next paragraph the flat spiral structure will be introduced based on this interaction and the field dependence for arbitrary temperatures according to Ref. [5] will be calculated.

The model used consists of N equidistant sublattices. In the following, the term sublattice refers to a trilayer defined above. The resulting magnetisation σ_n of each sublattice follows from Fig. 1. Without an external field the spin vectors stay in the plane. The free energy of this system looks like

$$F = -\sum_{n=1}^{N} B_1\sigma_n\sigma_{n+1} - \sum_{n=1}^{N} B_2\sigma_n\sigma_{n+2} - \cdots + g\mu_B H\sum_{n=1}^{N}\sigma_n. \quad (1)$$

Here, the exchange constants are labelled by B to be distinguished from the contents of MFA-results in Ref. [7]. The single-spin orientations are characterised through the angle φ_n between the spin and the external field, which is oriented parallel to the planes. Eq. (1) can be rewritten as

$$F = -B_1\sum_n \sigma^2\cos(\varphi_{n+1}-\varphi_n) - B_2\sum_n \sigma^2\cos(\varphi_{n+2}-\varphi_n) - \cdots + g\mu_B H\sigma\sum_n \cos\varphi_n. \quad (2)$$

Minimising this energy (with the boundary condition $\varphi_N = \varphi_0$), one solution for zero external field is

$$\varphi_{n+1}-\varphi_n = q_0 = \text{const.},$$
$$-\tfrac{1}{2}B(q_0) = -B_1\cos(q) - B_2\cos(2q). \quad (3)$$

The strength of the exchange interaction normally decreases very quickly with distance, so only the first two exchange constants are taken into account. Under this assumption three types of solutions are possible: a ferromagnetic ($q_0 = 0$), an antiferromagnetic ($q_0 = \pi$) and a screw solution,

$$\cos(q_0) = -\frac{B_1}{4B_2}, \quad \left|\frac{B_1}{4B_2}\right| < 1. \quad (4)$$

The ferromagnetic and antiferromagnetic solutions are only special cases of the general case of

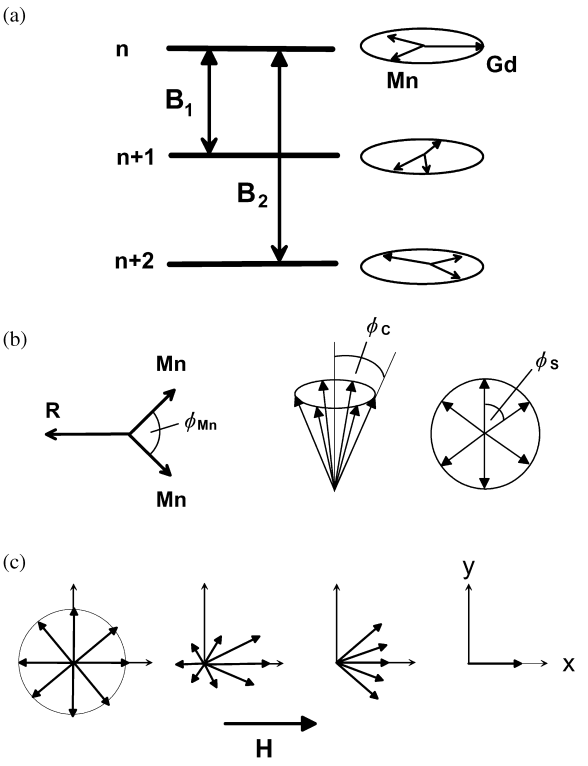

Fig. 1. Spiral spin structures of $Gd_XY_{1-X}Mn_6Ge_6$: (a) stacking of Gd and Mn layers and exchange constants considered in the spiral model. n means a unit of two Mn sublattices and one Gd sublattice. (b) Definition of characteristic angles in the spiral system. (c) Assumed arrangement of the trilayer sublattice magnetisations according to Eq. (18).

spiral structures. For zero temperature the angle φ_n can be rewritten as

$$\varphi_n = nq + \alpha + \varepsilon_n \quad \text{with} \quad \sum_n \varepsilon_n = 0. \tag{5}$$

The development of the energy (2) up to fourth order gives

$$\sum_{i=0}^{4} \frac{F_i}{N} = -\frac{1}{2}B(q) - \frac{1}{2}\frac{\mu_B^2}{2B(q) - B(2q) - B(0)}H^2 - \mu_B^4 \frac{[B(q) - B(2q)][B(q) - B(2q) + B(0)]}{[B(q) - B(3q)][2B(q) - B(2q) - B(0)]}H^4. \tag{6}$$

The term for the magnetisation consists of a term linear in H and a second term proportional to H^3.

$$m = -\frac{\partial}{\partial H}\sum_{i=1}^{4} \frac{F_i}{N} = a_1 H + a_2 H^3. \tag{7}$$

For $q = \pi$ and $= \pi/2$ there exists no exact solution because for these curves $[B(q) - B(3q)]$ is zero.

If the anisotropy energy is small in comparison with the exchange energy, the magnetisation of a sublattice $\mu_B\sigma$ can be described for any temperature through a Brillouin function

$$\mu_B\sigma = B\left(\frac{\mu_B H^m(\sigma, T)}{k_B T}\right), \tag{8}$$

$H^m(\sigma, T)$ represents the mean field for an arbitrary temperature. For zero field, σ should solve

$$\mu_B H^m(\sigma, T) = B(q_0)\sigma, \tag{9}$$

because of Eq. (3). If there is a field parallel to the sublattice plane, a mean field

$$\mu_B \boldsymbol{H}_n = \mu_B H^m(\sigma_n, T)\frac{\boldsymbol{\sigma}_n}{\sigma_n} = \mu_B \boldsymbol{H} + \sum_m B_{mn}\boldsymbol{\sigma}_m, \tag{10}$$

has an effect on the nth sublattice with the magnetic moment $\mu_B\sigma$. An alignment of all spins is reached at a saturation field of

$$\mu_B H_0 = [B(q_0) - B(0)]\sigma. \tag{11}$$

In comparison to normal mean-field calculations, here the mean field for arbitrary fields and temperatures possess a different value for each sublattice, which cannot be calculated analytically. But the value of the magnetisation in zero field ($\sigma_n = \sigma$) is known. We are able to develop $\mu_B H^m(\sigma_n, T)/\sigma_n$ around this value in powers of $(\sigma_n^2 - \sigma^2)$

$$\frac{\mu_B H^m(\sigma, T)}{\sigma_n} = \mu_B \frac{H^m(\sigma, T)}{\sigma} + \mu_B \frac{\partial}{\partial \sigma^2}\frac{H^m(\sigma, T)}{\sigma}(\sigma_n^2 - \sigma^2) + \cdots. \tag{12}$$

The first term corresponds to $B(q_0)$. To first order (10) gives a linear equation

$$B(q_0)\sigma_n = \mu_B H + \sum_m B_{mn}\sigma_m \tag{13}$$

with a characteristic general solution

$$\sigma_{nx} = \frac{\mu_B H}{B(q_0) - B(0)} + \zeta\sigma\cos(nq_0 + \alpha),$$
$$\sigma_{ny} = \eta\sigma\sin(nq_0 + \alpha) \tag{14}$$

The x-axis lies in the direction of the external field. The sum of ζ and η gives 1 for zero field. To calculate these amplitudes we need the second order of Eq. (12) and additionally a Fourier decomposition of Eq. (3):

$$\sigma_{nx} = \sigma[\zeta_0 + \zeta_1\cos(nq_0 + \alpha) + \zeta_2\cos[2(nq_0 + \alpha)] + \cdots],$$
$$\sigma_{ny} = \sigma[\eta_1\sin(nq_0 + \alpha) + \eta_2\sin[2(nq_0 + \alpha)] + \cdots]. \tag{15}$$

Because the single-Fourier components decrease, in this work all coefficients except of ζ_0, ζ_1 and η_1 can be neglegted. Inserting Eqs. (15) and (12) in Eq. (10) gives in second order

$$\mu_B\frac{\partial}{\partial^2\sigma}\left(\frac{H^m(\sigma, T)}{\sigma}\right)(\sigma_n^2 - \sigma^2)\frac{\sigma_{nx}}{\sigma} \simeq \frac{\mu_B H}{\sigma} - [B(q_0) - B(0)]\zeta_0,$$
$$\mu_B\frac{\partial}{\partial^2\sigma}\left(\frac{H^m(\sigma, T)}{\sigma}\right)(\sigma_n^2 - \sigma^2)\frac{\sigma_{ny}}{\sigma} \simeq 0. \tag{16}$$

The derivative of the mean field will be replaced by a temperature-dependent parameter

$$\gamma = \frac{2\mu_B \sigma^2}{B(q_0) - B(0)} \frac{\partial}{\partial \sigma^2}\left(\frac{H^m(\sigma, T)}{\sigma}\right). \tag{17}$$

A comparison of the coefficients of the trigonometric functions on both sides of Eq. (15) leads to a system of equations for the amplitudes ζ_0, ζ_1 und η_1 from this system. For the dependence of ζ_0 the following equations arise:

(i) fs-phase:
$$\zeta_0 \leqslant \frac{1}{2}, \quad \zeta_1^2 = 1 - 4\zeta_0, \quad \eta_1 = 1,$$
$$\left(1 + \frac{\gamma}{2}\right)\zeta_0 - \frac{5}{2}\gamma\zeta_0^3 = \frac{H}{H_0},$$

(ii) fs̃-phase:
$$\frac{1}{2} \leqslant \zeta_0 \leqslant 1, \quad \zeta_1 = 0,$$
$$\eta_1^2 = \frac{4}{3}(1 - \zeta_0)^2,$$
$$\left(1 - \frac{\gamma}{6}\right)\zeta_0 + \frac{\gamma}{6}\zeta_0^3 = \frac{H}{H_0}, \tag{18}$$

(iii) fm-phase:
$$\zeta_0 > 1, \quad \zeta_1 = \eta_1 = 0,$$
$$\left(1 - \frac{\gamma}{2}\right)\zeta_0 + \frac{\gamma}{2}\zeta_0^3 = \frac{H}{H_0}.$$

The nomenclature is flat spiral (fs), sinusoidal spiral (fs̃) and ferromagnetic (fm) spin structure. With small external fields we get a gradual alignment of the spins in the flat spiral structure in the direction of the external field. If γ is under a critical value of $\frac{8}{11}$ a continuous transition into a sinusoidal spin structure at a critical field of

$$H_{CF} = \left(\frac{1}{2} - \frac{\gamma}{16}\right)H_0 \tag{19}$$

is seen. If γ is greater than $\frac{8}{11}$, the transition is accompanied by a hysteresis loop.

The combination of macroscopic magnetisation data and NMR measurements yields the following arguments about the phase with lower magnetisation and at lower temperatures [7,8]:

- The total magnetisation of the $Gd_XY_{1-X}Mn_6Ge_6$ compounds disappears in zero field (Fig. 2).
- The local fields at the ^{155,157}Gd and the different ^{73}Ge sites lie in the plane perpendicular to the c-axis.
- The temperature dependence of the ^{73}Ge and ^{55}Mn hyperfine fields can be described within ferrimagnetic spin-wave theory. The temperature dependence of the ^{155,157}Gd hyperfine fields can be fitted with a ferromagnetic Brillouin function.
- The strong enhancement mechanism of these compounds is in contrast to an antiferromagnetic spin arrangement of the Mn and Gd sublattices.

Unifying all arguments together in one picture, we deduce the flat spiral spin structure shown in

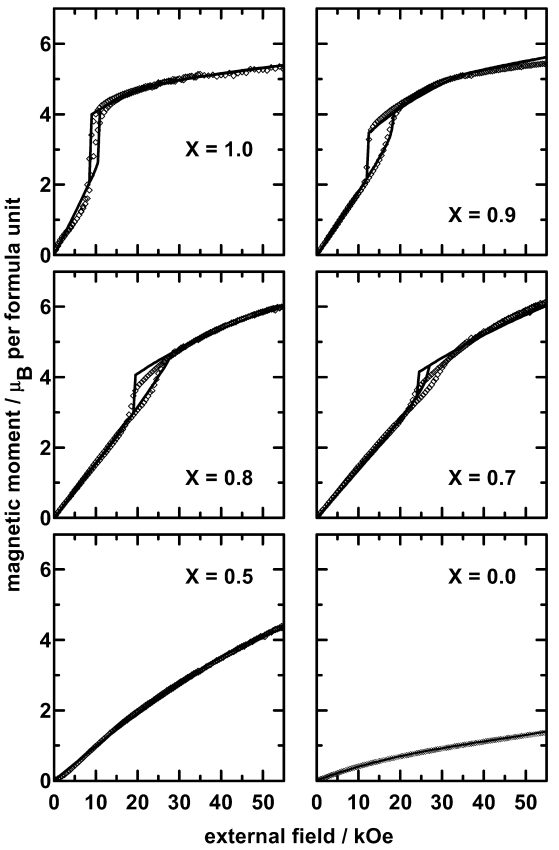

Fig. 2. Field dependence of the magnetisation of $Gd_XY_{1-X}Mn_6Ge_6$ powder samples at $T = 20$ K expressed as magnetic moment per formula unit. The solid lines are the results of a spiral spin model according to Eq. (18).

Table 1
Fit parameter of the flat spiral spin structure to the field dependence of the magnetic moment of the compounds $Gd_XY_{1-X}Mn_6Ge_6$. The critical fields for YMn_6Ge_6 are from Ref. [6]

X	σ/μ_B	H_{CF} (kOe)	$[B(q_0) - B(0)]$ (K)	γ (20 K)	B_1/B_2
1.0	5.0	0.90	0.24	4.79	—/—
0.9	5.7	1.46	0.34	5.13	—/—
0.8	6.4	2.15	0.45	6.08	—/—
0.7	7.1	2.60	0.49	6.20	—/—
0.0	12.0	15.0	1.68	—	4.84 K/ − 2.16 K

Fig. 1. The ferromagnetic Mn — but any angle smaller than 90° is also allowed between them — and Gd-sublattices build bigger trilayer sublattice sections (characterised with n in Fig. 1). This guaranties the disappearance of the total magnetisation in zero field and the linear trend in the macroscopic magnetisation at small fields according to Eq. (7).

If this assumption is right, the field dependencies of the $Gd_XY_{1-X}Mn_6Ge_6$ compounds should be described well with Eq. (18). The solid curves in Fig. 2 show a fit of the spiral structures with Eq. (18) in good agreement to the experimental values. In addition, it is shown that the hysteresis loops are the symptoms of an unsteady phase transition from a flat to a sinusoidal spin structure. Table 1 collects the chosen parameters for γ and H_{CT}. The magnetic moment $\sigma\mu_B$ per trilayer sublattice follows from $(6\mu_{Mn} - X\mu_{Gd})$. Only the difference $[B(q_0) - B(0)]$ is available because the spiral angle is not known from these types of measurements. But YMn_6Ge_6 offers a good comparison. Because in this substance not only the critical fields from high-field measurements are known [6] but also the spiral angle $\phi_S = 56°$ is known from neutron scattering [1]. On one hand, the tendency of $[B(q_0) - B(0)]$ to increase with lowering Gd concentration is confirmed. On the other hand, we are able to calculate in addition the exchange constants B_1 and B_2 from the spiral angle. The exchange constants have different signs in accordance with the oscillating character of the RKKY-interaction. In good agreement with neutron-scattering data, YMn_6Ge_6 possesses an antiferromagnetic interaction B_2 (Mn–Y–Mn) and a ferromagnetic interaction B_1 (Mn–Ge–Mn).

3. The phase diagrams of RMn_6Ge_6 (R = Tb, Dy)

If Gd is replaced by Tb, the ferrimagnetic-ordering temperature goes down to $T_C = 432$ K, shown in Fig. 3 for different field strengths. For $T_1 = 400$ K, a transition to a flat spiral spin structure (fs) starts off in nearly zero field (50 Oe), in good agreement to neutron-scattering data. This transition will be shifted to lower temperatures with increasing field strength favouring the ferrimagnetic range. The temperature dependence of the magnetic moment will be rather similar to the curves of $GdMn_6Ge_6$ [7]. Under $T_2 = 90$ K there is a third transition to a conic ferrimagnetic spin structure (cs) changing into the ferrimagnetic phase with increasing field strength. The field dependence of the magnetic moments in Fig. 4 allows a characterisation of the different spiral structures. The top picture shows the field dependence of the magnetic moment at $T = 10$ K. There are altogether three hysteresis loops whereby the middle one around zero field with a width of 40 Oe reflects a domain structure of the conic spin arrangement also seen in the temperature dependence. With the values $\phi_{Mn} = 17°$ and $\phi_C = 73°$ for the characteristic angles defined in Fig. 1 and known from neutron scattering [9], we get with a magnetic moment of $2.04\,\mu_B$ per Mn atom and $9\mu_B$ per Tb atom with

$$\mu_G = (6\mu_{Mn}\cos\phi_{Mn} - \mu_{Tb})\cos\phi_C, \tag{20}$$

the measured value of $0.78\,\mu_B$ for the axial moment at 200 Oe.

The other two hysteresis loops — lying symmetrically to zero field at about 20 kOe — mark in each case a phase transition from the conic spin arrangement (cs) to a sinusoidal spiral structure (cs̃) in the

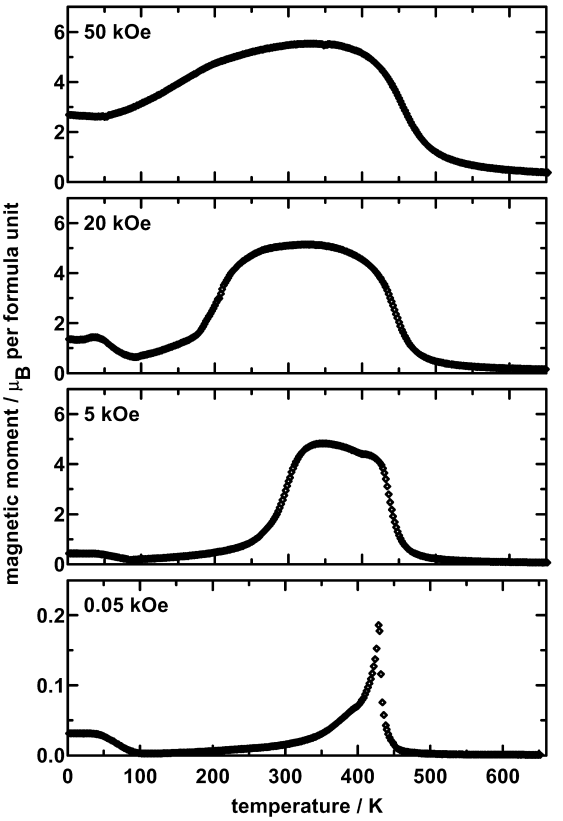

Fig. 3. Temperature dependence of the magnetisation of a $TbMn_6Ge_6$ powder sample at different fields expressed as magnetic moment per formula unit.

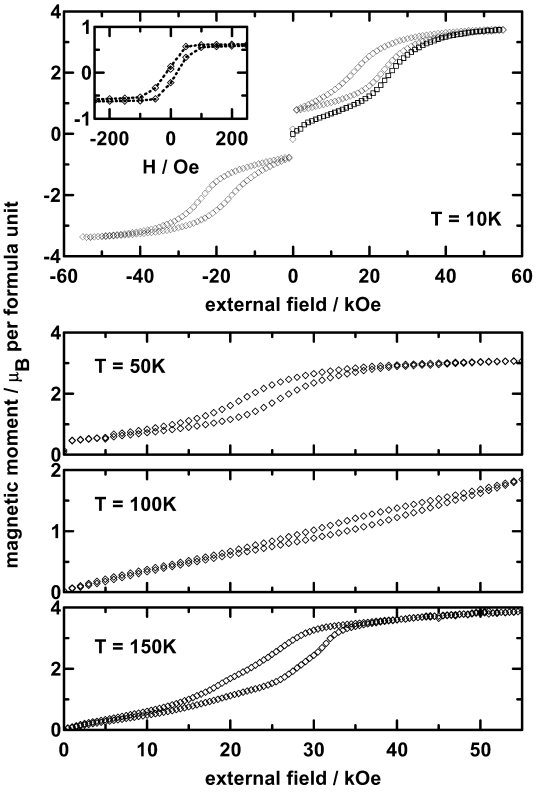

Fig. 4. Field dependence of the magnetisation of a $TbMn_6Ge_6$ powder sample at different temperatures expressed as magnetic moment per formula unit.

plane perpendicular to the c-axis. Parallel to the c-axis, only a continuous transition to a canted ferrimagnetic phase and a pure ferrimagnetic phase starting from a ferrimagnetic cone structure is possible.

At higher temperatures ($T = 50\,K$), ϕ_C goes to $\pi/2$ and μ_G decreases according to Eq. (20). In addition, the second hysteresis loop fades away at higher temperatures and disappears at T_2 ($T = 100\,K$ in Fig. 4). For temperatures above this temperature ($T = 150\,K$ in Fig. 4), the field dependence looks similar to the equivalent curves of $GdMn_6Ge_6$ (Fig. 2). In zero field the resulting magnetic moment disappears suggesting a similar spin structure as $GdMn_6Ge_6$. Neutron scattering detects a flat spiral structure in this temperature region [9]. After a linear increase up to 12 kOe there exists a phase transition from the flat into a sinusoidal spin structure (fs̃). For higher fields the magnetic moment continuously tends to a ferrimagnetic phase after a canted ferrimagnetic phase.

Similar to the previous compound, $DyMn_6Ge_6$ also possesses two ordering temperatures. While at $T_N = 427\,K$ an antiferromagnetic ordering (af) takes place (Fig. 5), this one passes over to a ferrimagnetic ordering (fi) at $T_C = 350\,K$ not yet seen in neutron scattering [10]. After a decrease of the magnetic moment in a flat spiral structure at $T_1 = 258\,K$, there is — similar to $TbMn_6Ge_6$ — an increase of the magnetic moment into a ferrimagnetic conic structure for temperatures under $T_2 = 56\,K$. Higher fields favour the ferrimagnetic phase and the antiferromagnetic phase becomes smaller but not zero even at 50 kOe. This is in accordance to high-field measurements [6]. There

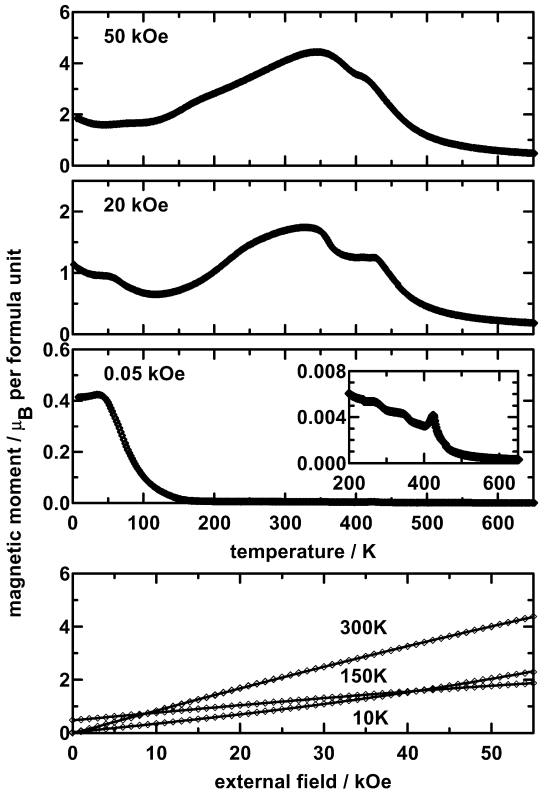

Fig. 5. Temperature dependence of the magnetisation of a $DyMn_6Ge_6$ powder sample at different fields expressed as magnetic moment per formula unit. The lower picture shows the field dependence of the magnetisation at different temperatures expressed as magnetic moment per formula unit. The solid lines are the results of a spiral spin model.

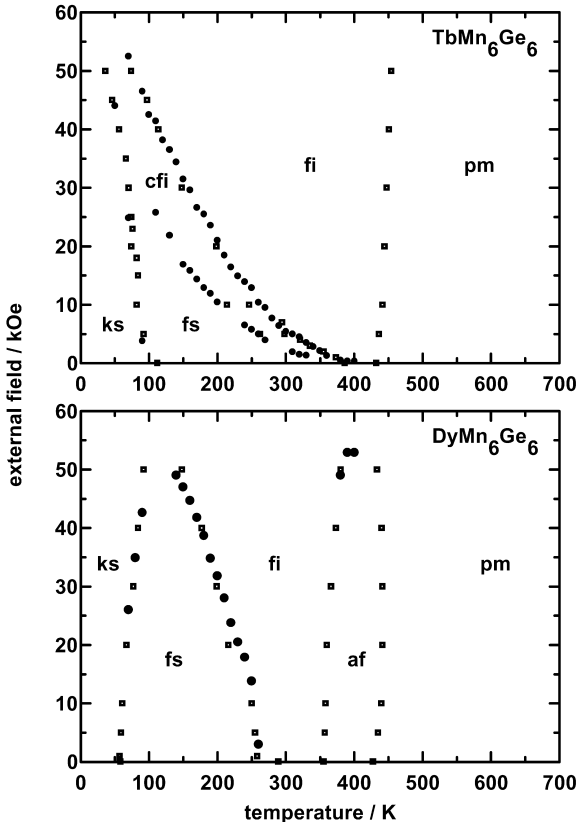

Fig. 6. Magnetic phase diagrams of $TbMn_6Ge_6$ and $DyMn_6Ge_6$ with paramagnetic (pm), ferrimagnetic (fi), antiferromagnetic (af), canted ferrimagnetic (cfi), conical spin (ks) and flat spiral spin phases (fs).

$DyMn_6Ge_6$ shows a much higher transition field in comparison to the magnetic moments of $TbMn_6Ge_6$ already aligned parallel to the external field at 50 kOe.

The assumption of a conic ferrimagnetic spin arrangement at low temperatures can be confirmed by the field dependence of the magnetic moment at 10 K. The curve does not go through zero field. Similarly $TbMn_6Ge_6$, one deduces from the measured values for the angles [10] $\phi_{Mn} = 20^\circ$ and $\phi_C = 57^\circ$ and a low-field moment of $0.45\mu_B$, a magnetic moment of $1.93\mu_B$ per Mn atom and $10\mu_B$ per Dy moment according to Eq. (20). At higher temperatures the field dependent magnetisation curve goes similar to $TbMn_6Ge_6$ through zero but not with a hysteresis loop.

Fig. 6 shows the magnetic phase diagrams of both compounds with their different magnetic spin structures. The phase boundaries have been deduced for continuous phase transitions from the point of maximum curvature on the $M(T)$ or $M(H)$ curve. For discontinuous phase transitions the point of maximum slope was used.

Therefore, in comparison to $GdMn_6Ge_6$, compounds with heavier rare-earths ions (R = Tb, Dy) possess a conic spin structure in addition to the flat spiral structure. This extra phase transition can be explained by the crystal field of these compounds produced by the rare earths [11]. It is quite difficult to make any suggestions for the crystal-field parameter because until now there exist only powder samples. But without the

Table 2
Exchange constants of the RMn_6Ge_6 (R = Y, Tb, Dy) compounds calculated from critical fields [6] and the spiral angles [1,10,9] of these compounds. T gives the temperatures, at which the values are measured.

R	T (K)	H_0 (kOe)	σ/μ_B	B_1 (K)	B_2 (K)	$[B(q_0) - B(0)]$ (K)
Y	2	30	12.0	4.84	− 2.16	1.68
Tb	2	5	3.74	6.07	− 2.22	0.90
Dy	10	20	3.50	7.97	− 3.85	3.84

knowledge of this parameter, it seems impossible to explain the complicated temperature dependence accurately. Nevertheless the field dependence of $DyMn_6Ge_6$ could be fitted according to Eq. (7).

Finally, and as comparison to the fitted values for $Gd_XY_{1-X}Mn_6Ge_6$, the exchange constants B_1 and B_2 and the values for $[B(q_0) - B(0)]$ for the RMn_6Ge_6 are calculated in Table 2 according to Eqs. (4) and (11).

4. Concluding remarks

The assumption of localised spin moments for Mn sites in these compounds is confirmed by a quantitative and qualitative analysis of experimental data. Band-structure calculations are in progress in order to gain further theoretical understanding of the local moments. The complicated spiral spin structures of the heavy RMn_6Ge_6 can be well described within a modified mean-field calculation. The assumption of a flat spiral spin structure in the low-field region of $Gd_XY_{1-X}Mn_6Ge_6$ given by combined arguments of the macroscopic view of magnetisation measurements and the microscopic view of nuclear magnetic resonance are confirmed.

Acknowledgements

We thank the Deutsche Forschungsgemeinschaft for financial support.

References

[1] G. Venturini, R. Welter, B. Malaman, E. Ressouche, J. Alloys Compounds 200 (1993) 52.
[2] J.H.V.J. Brabers, V.H.M. Duijn, F.R. de Boer, K.H.J. Buschow, J. Alloys Compounds 198 (1993) 127.
[3] P. Rösch, M.T. Kelemen, B. Pilawa, E. Dormann, K.H.J. Buschow, J. Magn. Magn. Mater. 164 (1996) 175.
[4] T. Nagamiya, K. Nagata, Y. Kitano, Progr. Theoret. Phys. 27 (1962) 1253.
[5] Y. Kitano, T. Nagamiya, Progr. Theoret. Phys. 31 (1964) 1.
[6] J.H.V.J. Brabers, Q.A. Li, F.R. de Boer, K.H.J. Buschow, IEEE Trans. Magn. 30 (1994) 1190.
[7] M.T. Kelemen, P. Rösch, E. Dormann, K.H.J. Buschow, J. Magn. Magn. Mater. 188 (1998) 195.
[8] P. Rösch, M.T. Kelemen, E. Dormann, G. Tomka, P.C. Riedi, J. Phys.: Condens. Matter 12 (2000) 1065.
[9] P. Schobinger-Papamantellos, J. Rodriguez-Carvajal, G. André, K.H.J. Buschow, J. Magn. Magn. Mater. 150 (1995) 311.
[10] P. Schobinger-Papamantellos, J. Schefer, J.H.V.J. Brabers, K.H.J. Buschow, J. Alloys Compounds 215 (1994) 111.
[11] M.T. Kelemen, Magnetische Ordnung und Hyperfeinwechselwirkung in ternären Seltenerd-Mangan-Germanium-Verbindungen, Ph.D. Thesis, Universität Karlsruhe (TH), and Cuvillier Verlag Göttingen, 1999.